ACCSCIENCE PUBLISHING

Journal of Energy and Sustainability

ORIGINAL RESEARCH ARTICLE

Influence of illumination on eco-friendly titanium dioxide/epoxy nanocomposite-based triboelectric nanogenerators

Prabhakar Yadav[1], Kuldeep Sahay[1]*, Arpit Verma[2], Bal Chandra Yadav[2]*, Yurii S. Bukichev[3], and Gulzhian I. Dzhardimalieva[3]

[1]Department of Electrical Engineering, Institute of Engineering and Technology, A. P. J. Kalam Technical University, Lucknow, Uttar Pradesh, India

[2]Nanomaterials and Sensors Research Laboratory, Department of Physics, Babasaheb Bhimrao Ambedkar University, Lucknow, Uttar Pradesh, India

[3]Laboratory of Metallopolymers, Department of Polymers and Composite Materials, Federal Research Center of Problems of Chemical Physics and Medicinal Chemistry, Russian Academy of Sciences, Chernogolovka, Moscow, Russia

***Corresponding authors:**
Kuldeep Sahay
(kuldeep.sahay@ietlucknow.ac.in)
Bal Chandra Yadav
(balchandra_yadav@rediffmail.com)

Citation: Yadav P, Sahay K, Verma A, Yadav BC, Bukichev YS, Dzhardimalieva GI. Influence of illumination on eco-friendly titanium dioxide/epoxy nanocomposite-based triboelectric nanogenerators. *Journal of Energy and Sustainability*. 2025;1(2):025140002. doi: 10.36922/JES025140002

Received: April 5, 2025

1st revised: June 29, 2025

2nd revised: October 22, 2025

Accepted: November 10, 2025

Published online: December 30, 2025

Abstract

Triboelectric nanogenerators (TENGs) based on titanium dioxide (TiO_2)/epoxy nanocomposites have attracted increasing interest as self-powered systems capable of harvesting mechanical friction and light energy for sustainable electricity generation. In this study, a photoinduced TENG was developed using TiO_2/epoxy nanocomposites with a polyethylene terephthalate charge collector. Scanning electron microscopy and X-ray diffraction analyses were conducted to evaluate the structural and morphological properties of the nanocomposite, revealing the presence of TiO_2 nanoparticles with an anatase crystal structure. Ultraviolet–visible spectroscopy was employed to investigate the optical properties of the nanocomposite, identifying an optical band gap energy of 3.52 eV. In addition, Fourier transform infrared spectroscopy was used to determine chemical bonds and functional groups. Epoxy serves as the matrix material, binding the TiO_2 nanoparticles and providing mechanical integrity to the composite film. It ensures uniform dispersion of TiO_2 nanoparticles and offers a flexible yet robust substrate essential for the repeated contact–separation cycles of TENG operation. The TiO_2/epoxy nanocomposite, used as the electrode for the TENG device, was created by incorporating TiO_2 nanoparticles into the epoxy resin. Without ultraviolet illumination, the TENG devices generated output voltages of 25, 45, 50, and 55 V at TiO_2 concentrations of 0, 2, 3, and 4 wt%, respectively. Under ultraviolet illumination, the corresponding voltages increased to 65, 75, 77, and 80 V. The highest voltage of 80 V was obtained for the device containing 4 wt% TiO_2. These findings provide valuable insights into the structural, morphological, optical, and chemical characteristics of the nanocomposite, supporting the development of effective and sustainable power sources.

Keywords: Triboelectric nanogenerator; Photoinduced triboelectric nanogenerator; Titanium dioxide/epoxy nanocomposite; Solution blending technique; Power sources

1. Introduction

Mechanical energy, such as motion or friction, can be converted into electrical energy using an energy-harvesting device known as a triboelectric nanogenerator (TENG). The term "triboelectric effect" refers to the movement of charges between two materials when they come into contact and subsequently separate.[1-3] Utilizing nanomaterials in the design of TENGs can improve their performance. Among these materials, titanium dioxide (TiO_2) is widely used in many applications due to its unique properties.[4-6] When integrated as a functional layer within the TENG structure, TiO_2-based composites can further improve energy-conversion efficiency.[7,8] Electron–hole pairs are produced when light interacts with TiO_2 nanoparticles; these charge carriers can then facilitate the triboelectric charging process if friction is applied to the composite material.[9-12] The interaction between light and friction enables the simultaneous harvesting of energy from both sources. The TiO_2/epoxy nanocomposite-based TENG offers several benefits for producing sustainable energy, as it can capture ambient light energy, making it suitable for interior settings or places with low light levels.[13-15] Parimalam *et al.*[16] investigated the organic-inorganic coatings utilizing bisphenol A diglycidyl ether, incorporating silica and other fillers via solution casting. TiO_2 and silicon dioxide nanoparticles enhanced the chemical resistance over 21 days, while the epoxy/silica/TiO_2/zinc oxide/latex nanocoating demonstrated outstanding heat resistance (efficiency of 90–99%) across various substrates. It is also possible to effectively transform the frictional energy produced by diverse mechanical actions into electrical energy. This capacity supports a wide range of applications, including harvesting energy from mechanical vibrations or human body movements.[17]

Through the provision of a self-powered system, nanocomposite-based TENGs can achieve energy self-sufficiency.[18-22] Although TiO_2/epoxy nanocomposites show strong potential for TENG applications, several challenges remain, including enhancing the durability and long-term stability of the materials, fine-tuning the nanocomposite composition, and improving the overall energy conversion efficiency.[23-25] Related studies demonstrate the multifunctional advantages of composite fillers. For example, epoxy/silica/TiO_2/zinc oxide coating demonstrated the highest bacterial reduction (>95%) after 4 h.[26] The combined filler effect enhances stress, viscosity, and torque compared to individual fillers, suggesting potential industrial and medical applications in reducing microbial growth. TENGs employ TiO_2/epoxy nanocomposites to harness light and friction energy, providing a sustainable approach to electricity generation. Renewable reinforcements based on hydroxyapatite have been reported to improve the performance of biocomposite materials, and treated carbon black particles can increase the glass transition temperature and thermal decomposition resistance by 7°C.[27] Ongoing research continues to advance the performance and usability of these nanocomposite-based TENGs.[1,7,28]

The ability of TiO_2/epoxy nanocomposite-based TENGs to harvest energy simultaneously from light and mechanical friction makes them particularly promising. While frictional motion generates triboelectric charging, light energy absorbed by the TiO_2 nanoparticles contributes to the total charge generation.[29-31] These TENGs can generate electrical energy for low-power electronic devices without the need for external power sources by effectively harnessing ambient light sources, such as indoor illumination.[32-34] A previous study examined epoxy-based composite coatings containing 20 wt% colloidal nanosilica and varying amounts of microsized TiO_2 (5, 10, 15 wt%).[35] Fourier transform infrared (FTIR) spectroscopy confirmed the presence of functional groups, indicating a good interaction. Scanning electron microscopy (SEM) showed well-dispersed TiO_2 at lower loading. A higher percentage of TiO_2 resulted in enhanced absorption of ultraviolet (UV) light. In comparison to pure epoxy, nanocomposites showed an enhanced oxygen transport rate. To improve the total energy conversion efficiency of TENGs, current studies focus on optimizing electrode layout, device design, and the properties of nanocomposites. In addition, scaling up the production of TiO_2/epoxy nanocomposites and TENG devices in a cost-effective manner is receiving increasing attention to enable broader deployment.[36-38]

This work aims to develop polycondensed epoxy nanocomposites incorporating nitrogen-doped titanium dioxide (n-TiO_2) nanoparticles. The innovative aspect of this study lies in the creation of a TiO_2/epoxy nanocomposite deposited on a polyethylene terephthalate (PET) substrate for a photoinduced TENG.[32] This design expands the potential applications of nanogenerators and enables efficient harvesting of environmental energy. The epoxy matrix, enhanced with TiO_2 nanoparticles, was combined with the PET substrate, endowing the TENG with improved performance and unique functional properties. The device performance was examined at various TiO_2 concentrations (0 wt%, 2 wt%, 3 wt%, and 4 wt%), revealing that optimizing the TiO_2 content increased the voltage output, leading to a maximum voltage of 80 V.

2. Materials and methods

2.1. Materials

The materials used in this study included Kapton tape, double-sided copper tape, PET sheet (Techinstro, MH,

India), and double-sided tape. The epoxy matrix was based on the ED-20 resin. Diaminopentane (GOST 10587-84; Rearus LLC, Russia) was used as a hardener in the preparation of the TENG devices, with TiO_2 particles incorporated at 0, 2, 3, or 4 wt%. In the synthesis of the nanocomposite films, 4,4'-diaminodiphenylmethane (DDM; Sigma-Aldrich, United States; molar mass 198 g/mol, purity 97%) was used as the curing agent. The synthesized TiO_2 nanoparticles consisted of 75% anatase and 25% rutile with an average particle diameter of 46 nm. Dimethyldichlorosilane (HIMMED Trading House LLC, Russia) was employed as the surface treatment agent.

2.2. Synthesis procedure

Nanocomposites were prepared by sequentially curing ED-20 diane-epoxy resin at 90°C and 160°C in the presence of an aromatic hardener, with titanium(IV) dioxide nanoparticles synthesized via a plasma–chemical approach incorporated into the resin. Ultrasonic dispersion was employed to distribute the nanoparticles throughout the polymer matrix using a SONOREX Digital 10p ultrasonic bath (Bandelin, Sigma-Aldrich, United States). The ED-20 epoxy resin had a molecular weight of 385 and an epoxy group content of 22.6 wt%. DDM, produced by microwave-assisted synthesis, was used as the hardener. According to the process outlined by Bukichev *et al.*,[39] films of n-TiO_2/ED-20 epoxy resin can be prepared with TiO_2 concentrations ranging from 0.2 to 5 wt%. In this work, films containing 0, 2, 3, and 4 wt% TiO_2 were fabricated. To ensure correct stoichiometry, the TiO_2 nanoparticles were added to a mixture of ED-20 and DDM in an equimolar ratio of epoxy and amine groups, and dispersed for 20 min in an ultrasonic bath at 35 kHz. The mixture was treated with a toluene-based solution of dimethyldichlorosilane, which served as an anti-adhesive, and then cast into glass molds. A temperature-controlled oven was used to cure the samples using a stepped temperature regime of 90°C and 160°C each (3 h at each temperature), which, according to calorimetric data, ensured 95–97% curing. The resulting films had a thickness of 80–100 μm.

2.3. Device fabrication and experimental setup

The fabrication procedure for the TENG device is illustrated in Figure 1A, and the experimental setup is depicted in Figure 1B. The TENG structure was composed of PET sheets, copper tape (2 mm thick), Kapton tape (1 mm thick), double-sided foam tape, and an epoxy resin (ED20) cured with diaminopentane, with TiO_2 nanoparticles added at 0, 2, 3, or 4 wt%. Two copper tapes were attached to the PET sheets, serving as electrodes, with one electrode secured in place using Kapton tape. The surface of this Kapton tape was roughened using abrasive sandpaper to enhance the triboelectric effect. The second electrode was coated with the TiO_2/epoxy nanocomposite, where the TiO_2 heterostructure can strengthen the internal electric fields at the nanoparticle surfaces and increase the charge transfer rate between nanoparticles. The two contact layers were separated by double-sided foam tape spacers, each with an effective surface area of 24 cm^2. A Keithley 6517B electrometer (Tektronix/Keithley, USA) was used to measure variations in voltage.

2.4. Characterization methods

2.4.1. Scanning electron microscopy

Scanning electron microscopy was used to examine the surface morphology of the nanocomposite films. Before imaging, samples were sputter-coated with a thin gold layer to improve surface conductivity. SEM observations were performed using a JSM 6490 LV scanning electron microscope (JEOL, Japan) operated at an accelerating voltage of 20 kV. Micrographs were acquired at multiple magnifications.

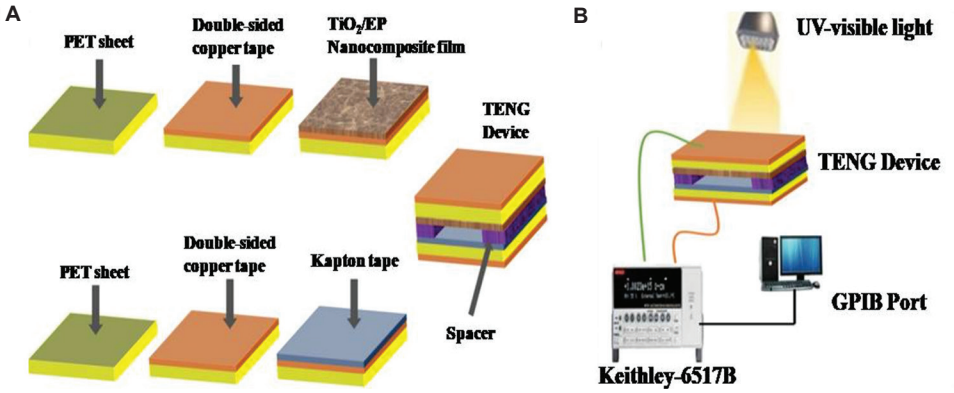

Figure 1. Fabrication of a TENG. (A) Fabrication steps of the TENG. (B) Experimental setup for testing the effect of ultraviolet–visible light. Abbreviations: EP: Epoxy; GPIB: General Purpose Interface Bus; PET: Polyethylene terephthalate; TENG: Triboelectric nanogenerator.

2.4.2. Energy-dispersive X-ray spectroscopy (EDS)

EDS was used to determine the elemental composition of the films. EDS analysis was performed using an INCAx-act EDS system (Model 51-1385-007, Oxford Instruments, Japan) integrated with the SEM, and spectra were processed using the INCA software package. Elemental spectra and point analyses (and/or elemental mapping, if performed) were collected to confirm the presence and distribution of constituent elements.

2.4.3. X-ray diffraction (XRD)

XRD patterns were collected using a Bruker D8 Advance diffractometer (Bruker, Germany) with Cu Kα radiation (λ = 1.5406 Å). Data were acquired over a 2θ range of 10–80° with a step size of 0.02° and a scan rate of 2° min^{-1}. Phase identification was performed by comparison with standard reference data (JCPDS/ICDD).

2.4.4. Ultraviolet–visible (UV–Vis) spectroscopy

UV–Vis absorbance spectra of the TiO_2/epoxy films were recorded using a Thermo Scientific Evolution 201 UV–Vis spectrophotometer (Japan) in the wavelength range of 200–800 nm with a data interval of 1 nm. Measurements were performed on film samples (thickness 80–100 µm), using using distilled water as the reference/baseline.

2.4.5. FTIR spectroscopy

FTIR spectra were acquired using a Thermo Scientific Nicolet 6700 FTIR spectrometer (USA). Spectra were recorded in the range of 200–800 nm at a resolution of 0.09 cm^{-1} with 36 scans per sample. Measurements were performed for TiO_2 nanoparticles and epoxy films containing 0, 2, 3, and 4 wt% TiO_2.

3. Results and discussion

3.1. Surface morphology

TiO_2 nanoparticles were dispersed throughout the epoxy matrix volume, both as individual particles and aggregates, as determined by SEM measurements (Figure 2). The displayed histograms of the particle size distribution show that even at a relatively low concentration of nanofillers (0.5 wt%), the average diameter of particles in the original n-TiO_2 powder increased from 40 to 83 nm upon incorporation into the TiO_2/epoxy nanocomposite. Figure 2A shows the SEM image of pure epoxy resin, whereas Figure 2B-D shows the SEM images of 2 wt% n-TiO_2, 3 wt% n-TiO_2, and 4 wt% n-TiO_2 incorporated in the matrix of the epoxy resin samples. These SEM images clearly demonstrate the incorporation of TiO_2 nanoparticles into the epoxy matrix. Figure 2E and F depict the SEM images of the pure n-TiO_2 nanoparticles, which are spherical and range in size from

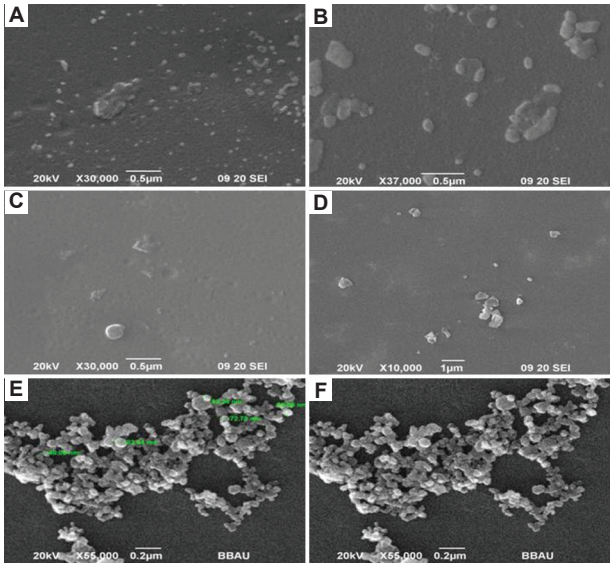

Figure 2. Scanning electron microscopy images of TiO_2/epoxy nanocomposite films. Images of films incorporated with (A) 0 wt%, (B) 2 wt%, (C) 3 wt%, and (D) 4 wt% n-TiO_2. Scale bars: 0.5 µm and 1 µm; magnifications: 10K×, 30K×, and 37K×. (E and F) Pure n-TiO_2 nanoparticles. Scale bar: 0.2 µm; magnification: 55K×.
Abbreviations: n-TiO_2: Nitrogen-doped titanium dioxide; TiO_2: Titanium dioxide.

10 to 100 nm. During curing, nanoparticle aggregation can lead to an increase in the effective size of the n-TiO_2 particles.

3.2. Energy dispersive spectroscopy analysis

Figure 3 presents the EDS spectra of epoxy resin with and without n-TiO_2, confirming the presence and weight percentage of titanium and oxygen. EDS was used alongside field-emission SEM to examine the chemical composition of the material. Figure 3A shows the EDS spectrum of 0 wt% TiO_2 epoxy, indicating the absence of titanium peaks. Figure 3B-D shows the EDS spectra of epoxy resin with 2 wt%, 3 wt%, and 4 wt% TiO_2, respectively, indicating the presence of titanium and carbon. According to the EDS analysis, the prepared TiO_2 exhibited distinct titanium and oxygen peaks while showing fewer contaminants, such as chlorine.

3.3. Structural analysis

Figure 4 depicts the X-ray diffraction pattern of the created TiO_2/epoxy composite film. According to Chen *et al.*,[40] the absence of spurious diffraction peaks indicates good crystallographic purity. The experimental data agree with the JCPDS card no. 00-015-0875, confirming the anatase phase of TiO_2. The 2θ at a peak of 25.4° confirms the TiO_2 anatase structure,[13] supported by additional strong peaks at 30.04° and 48°. No extraneous diffraction peaks were

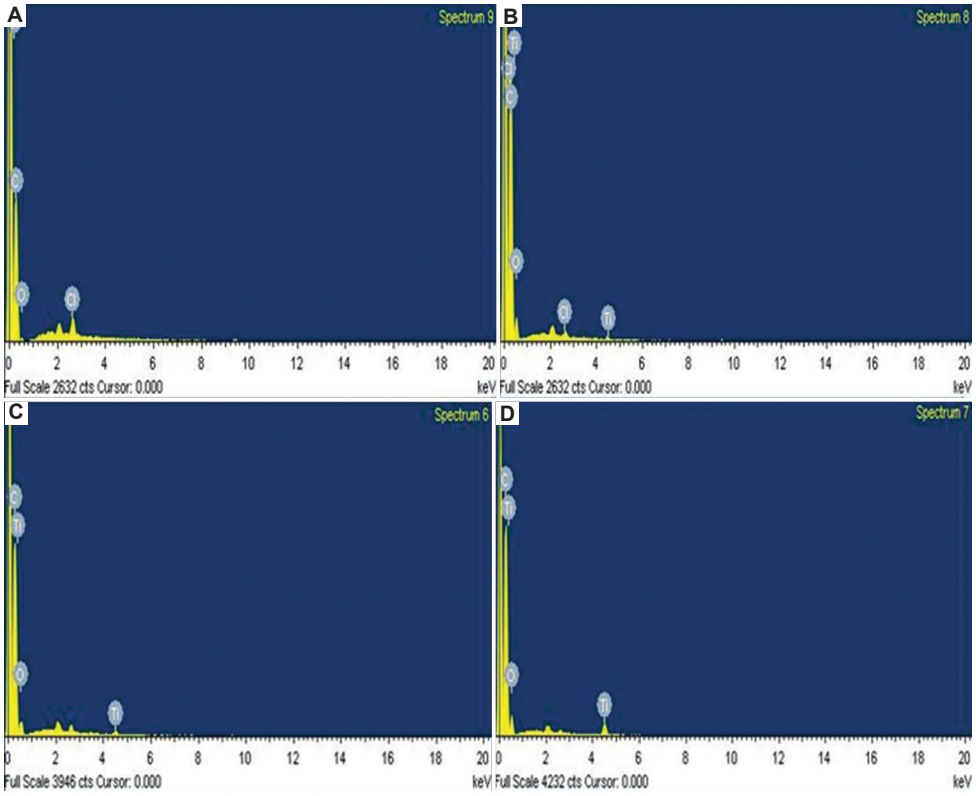

Figure 3. Energy dispersive spectroscopy spectrum and elemental compositions. Spectrum of epoxy with (A) 0 wt%, (B) 2 wt%, (C) 3 wt%, and (D) 4 wt% titanium dioxide.

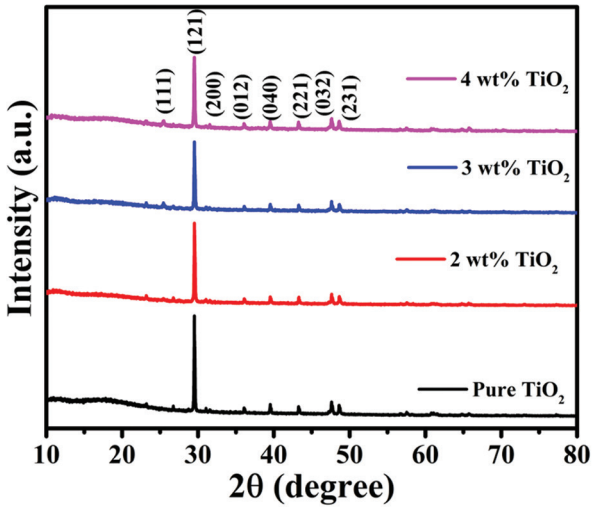

Figure 4. X-ray diffraction pattern of pure TiO_2 and epoxy composites of 2 wt%, 3 wt%, and 4 wt% TiO_2, respectively
Abbreviation: TiO_2: Titanium dioxide.

observed, indicating phase purity. The broad nature of the diffraction peaks suggests an extremely small crystallite size, while the overall peak intensities reflect the crystalline nature of the material.

3.4. UV–Vis absorption analysis

Figure 5A depicts the UV–Vis (300–1,200 nm) absorbance spectrum for the TiO_2/epoxy nanocomposite. The main absorption edge was observed at around 380 nm in the UV region. Tauc's plot was used to analyze the optical energy band gap value for the TiO_2/epoxy nanocomposite (inset in Figure 5B). The optical band gap (E_g) was calculated using Tauc's relation, as given by Equation 1:

$$\alpha = \frac{\alpha_0 \left(h\upsilon - E_g\right)^n}{h\upsilon} \quad (1)$$

where α_o is a characteristic parameter, α is the absorption coefficient, h is Planck's constant, and n is the power factor. Depending on the type of transition that occurred, the value of n may change. Since the transition in this nanocomposite material was direct, n is presumed to be 1/2. For the TiO_2/epoxy nanocomposite, the calculated value of E_g was 3.52 eV.

3.5. FTIR spectroscopy analysis

FTIR analysis of TiO_2 nanoparticles confirmed the formation of high-purity products. FTIR spectra (Figure 6) of these nanoparticles primarily display peaks associated

with TiO_2. A peak at 499.9 cm^{-1} is attributed to Ti–O stretching vibrations. The final product appeared to have Ti–O bonds and lacked OH or peroxo groups, as indicated by the FTIR spectrum. The produced TiO_2 nanoparticles' infrared spectra, which can be used to identify chemical bonds and functional groups in a product, were in the range of 400–4,000 cm^{-1}. Low-wavelength peaks at 585.6, 586.4, 566.9, and 565.1 cm^{-1} were assigned to C–I stretching vibrations. The highest peak observed for the TiO_2/epoxy nanocomposite in 0, 2, 3, and 4 wt% TiO_2 was 3,420.5, 3,403.3, 3,387.9, and 3,384.2 cm^{-1}, respectively, due to O–H stretching. In the low-energy region (<1,000 cm^{-1}), broad absorption bands associated with Ti–O stretching were observed. For the TiO_2/epoxy nanocomposite containing 0, 2, 3, and 4 wt% TiO_2, characteristic peaks appeared near 586 and 566 cm^{-1}.

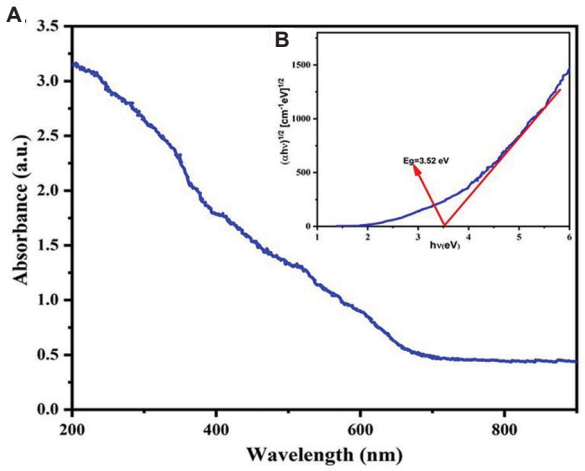

Figure 5. (A) Ultraviolet–visible spectrum of titanium dioxide/epoxy nanocomposite and (B) the Tauc's plot in the inset

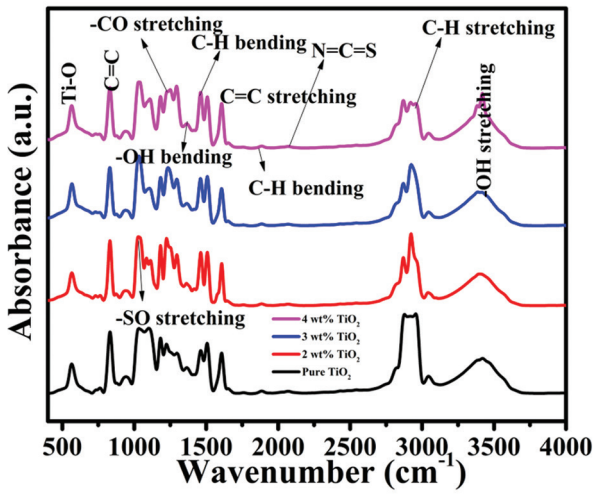

Figure 6. Fourier transform infrared analysis of TiO_2/epoxy nanocomposite of pure TiO_2 and epoxy of 2 wt%, 3 wt%, and 4 wt% TiO_2, respectively
Abbreviation: TiO_2: Titanium dioxide.

3.6. Experimental analysis for TENG devices

A TENG converts mechanical energy into electrical energy through the combined action of the triboelectric effect and electrostatic induction. It typically comprises two triboelectric layers made from materials with differing electron affinities. When these materials come into contact and then separate, one surface tends to gain electrons while the other loses them. Nylon, polytetrafluoroethylene, and polydimethylsiloxane are a few examples of frequently used triboelectric materials.[31] As seen in Figure 7A, electrodes on each side of the triboelectric layers collect the electrical charges generated during contact or separation. These electrodes are usually made of conductive materials, such as conductive polymers or metal foils. One electrode is attached to each triboelectric surface, enabling efficient charge collection.[7] The layers are often supported by a flexible substrate, such as a polymer film or a flexible printed circuit board, which provides both flexibility and structural stability. The electrical output of TENG may be utilized to charge batteries or power other devices. The electrodes are linked to an external load, such as a resistor or energy storage device, completing the electrical circuit and enabling practical energy utilization. To enable the creation of mechanical energy, the TENG device may incorporate various mechanical structures. The overall fabricated TENG device is shown in Figure 7A, while the photographic images of the fabricated TENG and

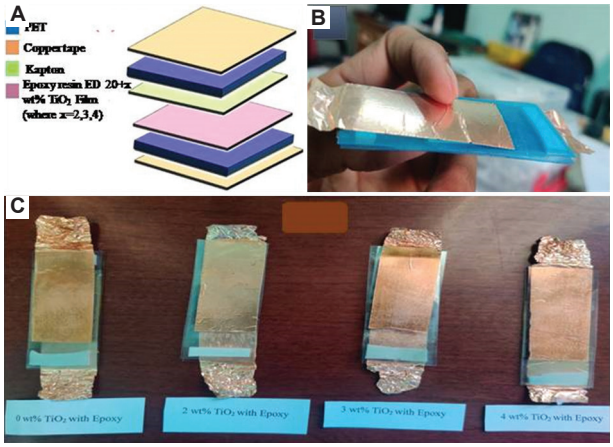

Figure 7. Device fabrication. (A) Constituent layers in epoxy resin TiO_2-based TENGs. (B) Image of fabricated TENG. (C) Images of fabricated TENG with TiO_2/epoxy nanocomposite films incorporated with 0 wt%, 2 wt%, 3 wt%, and 4 wt% n-TiO_2, respectively.
Abbreviations: n-TiO_2: Nitrogen-doped titanium dioxide; TENG: Triboelectric nanogenerator; TiO_2: Titanium dioxide.

TiO_2/epoxy nanocomposite-based devices with varying TiO_2 concentrations are presented in Figures 7B and C, respectively.

The optimized output voltage characteristics of the TENG device without UV light irradiance are presented in Figure 8. The TENG device produced a voltage of 25 V using 0 wt% TiO_2 nanoparticles, as shown in Figure 8A. Under triboelectric operation, this device exhibits the smallest electrical potential difference between its electrodes. Nonetheless, even at this lower voltage, the device is capable of generating a measurable charge flow. The TENG device containing 2 wt% TiO_2 nanoparticles generated a higher voltage of 45 V compared to the sample containing 0% TiO_2 (Figure 8B). This implies that the inclusion of TiO_2 nanoparticles increased the electrical potential difference. In comparison to the two prior samples, the TENG device with 3 wt% TiO_2 nanoparticles produced a voltage of 50 V (Figure 8C). This suggests that increasing the concentration of TiO_2 nanoparticles leads to a larger electrical potential difference and enhances charge transfer within the system. The TENG device with 4 wt% TiO_2 nanoparticles generated a voltage of 55 V (Figure 8D), the highest among all the samples. This indicates that higher TiO_2 loading is associated with a larger electrical potential difference and a greater charge flow. Although it is slightly lower than the earlier samples, it remains in the same ballpark, indicating a sizable flow of electrical charges. Voltages usually increase as TiO_2 nanoparticle concentration rises, indicating an increase in electrical potential differences.[40,41] TiO_2 nanoparticles possess unique properties that enhance the performance of nanogenerators. They are wide-bandgap semiconductor materials that effectively transform light energy into electrical energy. Their inclusion expands the surface area, creating a network of connections that improves electrical conductivity, electron mobility, and charge transfer. When materials with various electron affinities come into contact, TiO_2 nanoparticles enhance the triboelectric effect by acting as electron acceptors and donors. This makes charge transfer easier, which raises the output voltage. In addition, TiO_2 nanoparticles strengthen the epoxy matrix, improving its flexibility, toughness, and resistance to mechanical stress. TiO_2/epoxy nanocomposite-based photoinduced TENGs exhibit improved performance and durable power production capabilities due to these combined features.

The optimized output voltage characteristics of the TENG device under UV light irradiance are presented in Figure 9. Table 1 compares the output voltage characteristics of the TENG device with and without UV light, showing a drastic increase in the output voltage of the TENG devices. When exposed to UV light, the TENG device with 0 wt% TiO_2 nanoparticles produced a higher voltage of 65 V (Figure 9A) compared to the corresponding device operated without UV illumination, as presented in Figure 9B. The electrical potential difference in this sample appears to be amplified by UV light irradiation. Under UV light irradiation, the TENG device with 2 wt% TiO_2 nanoparticles generated a voltage of 75 V (Figure 9B). This implies that the electrical potential difference was higher than it was in the UV-free sample. With 3 wt% TiO_2 nanoparticles and UV light irradiation, the TENG device generates a voltage of 77 V (Figure 9C). The voltage in this sample was slightly higher than previously reported ones.[42] When subjected to UV light, the TENG device with 4 wt% TiO_2 nanoparticles produced the highest voltage of 80 V among all the samples (Figure 9D). This indicates that the largest electrical potential difference

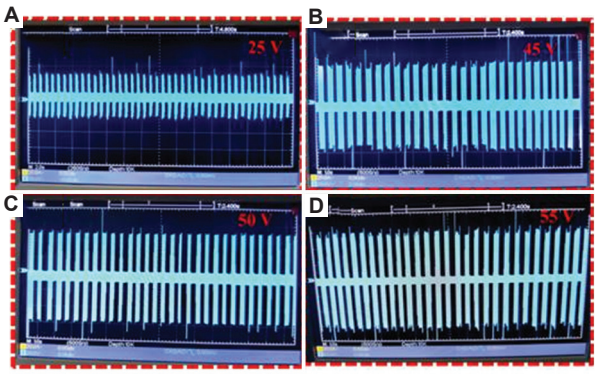

Figure 8. Characteristics of TiO_2/epoxy nanocomposite-based triboelectric nanogenerators without ultraviolet light exposure. Output voltage for (A) 0 wt%, (B) 2 wt%, (C) 3 wt%, and (D) 4 wt% TiO_2, respectively.
Abbreviation: TiO_2: Titanium dioxide.

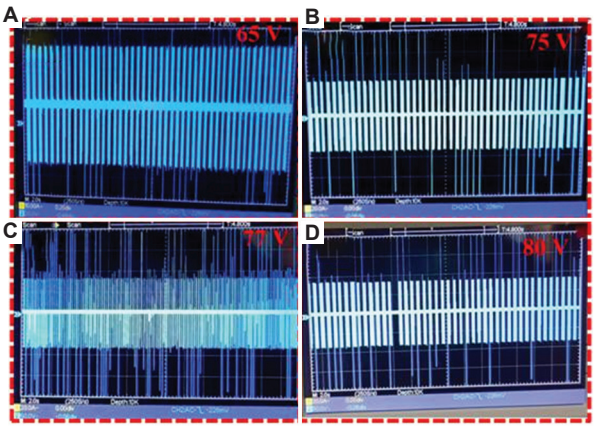

Figure 9. Characteristics of TiO_2/epoxy nanocomposite-based triboelectric nanogenerators with ultraviolet light exposure. Output voltage for (A) 0 wt%, (B) 2 wt%, (C) 3 wt%, and (D) 4 wt% TiO_2, respectively.
Abbreviation: TiO_2: Titanium dioxide.

occurred when UV light irradiation and TiO_2 nanoparticle concentration are combined. UV light illumination led to an increased generation of electrical charges. The TENG device performed better when UV light irradiance was added together with different TiO_2 nanoparticle concentrations. For all compositions, UV illumination increased the voltage output. The current output remained relatively constant for most samples, except for the device containing 4 wt% TiO_2, which exhibited a substantial increase in current under UV light. These findings suggest that UV light, particularly when combined with precise concentrations of TiO_2 nanoparticles, can enhance the generation of electrical energy in TENG devices. The triboelectric voltage produced in the samples is greatly influenced by UV radiation. When UV light irradiates TiO_2 nanoparticles, it activates the photovoltaic effect. Due to its wide bandgap, TiO_2 can absorb photons in the UV region, leading to the generation of electron–hole pairs. Upon photon absorption, electrons are excited to higher energy levels, leaving behind positively charged holes. This charge separation creates an internal electric potential, resulting in a built-in voltage across the material.[43] This built-in voltage influences the total triboelectric voltage measured. The TiO_2 nanoparticles can be used to produce electron–hole pairs, which can enhance the triboelectric effect. The triboelectric effect occurs when two materials with differing electron affinities, such as the opposing substance and the TiO_2 nanoparticles, come into contact. The opposing material may absorb the excited electrons from the TiO_2 nanoparticles, thereby enhancing the charge density and triboelectric voltage.

3.7. Mechanism of TENGs

The mechanism can be understood as follows: when two dielectric materials, Kapton and a TiO_2/epoxy nanocomposite, come into contact, electrification occurs, resulting in the formation of opposite static charges on the inner surfaces of the triboelectric layers. Upon separation of these layers, a potential difference is created, causing electrons to flow under short-circuit conditions.[44] A charge imbalance develops between two materials that have different electron affinities when they come into contact and then separate, creating an electric potential.[45] TiO_2 nanoparticles are well known for their superior electrical and optical characteristics, which make them suitable for use in energy-related applications. The PET substrate serves as the foundation material for the nanocomposite, providing mechanical flexibility, toughness, and insulation. In this instance, inherent motion or deformation of the device provides the mechanical energy needed for the triboelectric effect. The photoinduced mechanism indicates that light can activate or enhance the performance of the nanogenerator.[23] TiO_2 is a semiconductor with photoactive characteristics, meaning that when exposed to light, it can produce electron–hole pairs. The photoactive characteristics of TiO_2 nanoparticles play a role in the reaction of TENG to UV radiation. Because TiO_2 nanoparticles in the anatase phase are photocatalytic, they produce electron–hole pairs when exposed to UV light. Figure 10 illustrates the role of UV light on the enhanced characteristics of TiO_2/epoxy nanocomposite-based TENG. On the TiO_2/epoxy composite, these electron–hole pairs improve charge separation and increase surface charge density. The TENG produces more voltage as a result of the enhanced triboelectric effect caused by this greater charge density. Higher concentrations of TiO_2 produce higher voltage output as they enhance the material's capacity to capture and transmit charges more effectively when exposed to UV light. By enhancing charge transfer during contact and separation, these charge carriers can support the triboelectric effect and increase the total electrical output of the nanogenerator.[46] Moreover, the incorporation of TiO_2 nanoparticles into the epoxy matrix can also influence the surface morphology and interfacial properties of the nanocomposite. This can lead to improved contact electrification and charge transfer efficiency, further enhancing the voltage output of the TENG device. During the deformation process, the TiO_2/epoxy nanocomposite layer and the PET substrate

Table 1. Output voltage of the triboelectric nanogenerator devices with and without UV light

Sample wt% of titanium dioxide	Without UV light	With UV light
0	25 V	65 V
2	45 V	75 V
3	50 V	77 V
4	55 V	80 V

Abbreviation: UV: Ultraviolet

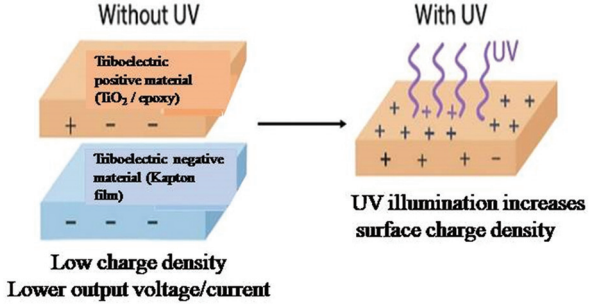

Figure 10. Impact of UV light on the charge density of TiO_2/epoxy nanocomposite-based triboelectric nanogenerator
Abbreviations: TiO_2: Titanium dioxide; UV: Ultraviolet.

come into contact and eventually separate due to the subsequent application of pressure. The triboelectric effect is produced by the contact and separation process. The TiO_2/epoxy nanocomposite layer and the PET substrate transmit electrons due to the triboelectric phenomenon, and between the two materials, this charge transfer produces an electric potential. Through the use of proper electrodes and electronics that are attached to the device, the created electric potential can be harnessed and collected.[34] By applying UV light, TiO_2 nanoparticles in the nanocomposite layer can absorb photons and produce additional charge carriers. The triboelectric effect is enhanced by this photoinduced action, resulting in increased electrical output.[47,48] The triboelectric interaction between the TiO_2/epoxy nanocomposite layer and the PET substrate can be exploited in a self-powered, photoinduced TENG to convert mechanical energy into electrical energy.[49] The charge transfer process during contact and separation can therefore be facilitated by these photoexcited charge carriers, increasing the total electrical output of TENG. The operating range of TiO_2-based TENGs can be extended by UV light, which acts as a supplementary energy source.[50,51] The TENG device can capture energy from both mechanical motion and UV illumination in its surroundings, utilizing visible or UV light, enabling it to function autonomously even with modest mechanical stimulation. It is a prospective contender for several applications, including wearable technology, self-powered sensors, and energy harvesting from ambient light sources due to its dual-mode energy-collecting capacity. Comparison with previously reported devices indicates that most earlier studies achieved higher output voltages[48-50] than those obtained here, with the exception of Alam *et al.*[52] However, to the best of our knowledge, none of these studies systematically examined the effect of UV illumination on TENG performance, which is the key innovation of the present work.

4. Conclusion

This study used a TiO_2/epoxy nanocomposite-blended PET substrate to create a photoinduced TENG. Structural and morphological investigations revealed the presence of TiO_2 nanoparticles with anatase crystal structure in the nanocomposite. The performance of the TENG device was examined under the effect of UV light, and the findings indicated that varying TiO_2 concentrations had an impact on the output voltage. The device containing 4 wt% TiO_2 produced the highest voltage output of 80 V under UV illumination. For the device without TiO_2 (0 wt%), the voltage increased from 25 V (without UV) to 65 V under UV illumination. These results provide important new insights into the structural, morphological, optical, and chemical properties of the blended TiO_2/epoxy nanocomposite PET substrate. The development of such self-powered, photoinduced TENGs may significantly advance sustainable power-source technologies. Environmental stimuli, such as UV light, can thus be exploited to generate energy, paving the way for self-sufficient and portable energy-generating systems. Future studies can focus on maximizing the TiO_2 concentration and exploring other materials to enhance TENG performance.

Acknowledgments

The authors acknowledge the USIC, Babasaheb Bhimrao Ambedkar University, Lucknow, U.P., India, for providing the characterization facilities. G.I. Dzhardimalieva and Y.S. Bukichev acknowledge the Federal Research Center of Problems of Chemical Physics and Medicinal Chemistry of the Russian Academy of Sciences (state registration 124013000757-0).

Funding

None.

Conflict of interest

The authors declare that they have no competing interests

Author contributions

Conceptualization: Yurii S. Bukichev
Formal analysis: Arpit Verma
Investigation: Prabhakar Yadav
Methodology: Prabhakar Yadav
Supervision: Kuldeep Sahay, Bal Chandra Yadav
Validation: Bal Chandra Yadav
Writing–original draft: Prabhakar Yadav
Writing–review & editing: Arpit Verma, Bal Chandra Yadav, Gulzhian I. Dzhardimalieva

Ethics approval and consent to participate

Not applicable.

Consent for publication

Not applicable.

Availability of data

Data will be available from the corresponding authors upon reasonable request.

References

1. Basu R, Iannacchione GS. Dielectric response of multiwalled carbon nanotubes as a function of applied ac-electric fields. *J Appl Phys.* 2008;104(11):114107.

doi: 10.1063/1.3035963

2. Chaturvedi AK, Badatya S, Pappu A, Srivastava AK, Gupta MK. Sustainable robust waste-recycled ocean water-resistant fly ash-carbon nanotube nanocomposite-based triboelectric nanogenerator. *Sustain Energy Fuels.* 2023;7(7):1735-1746.

doi: 10.1039/D2SE01698B

3. Homes CC, Vogt T. Doping for superior dielectrics. *Nat Mater.* 2013;12(9):782-783.

doi: 10.1038/nmat3744

4. Ioannou G, Patsidis A, Psarras GC. Dielectric and functional properties of polymer matrix/ZnO/$BaTiO_3$ hybrid composites. *Compos Part A Appl Sci Manuf.* 2011;42(1):104-110.

doi: 10.1016/j.compositesa.2010.10.003

5. Jannesari M, Asadian E, Ejehi F, *et al.* Boosting on-demand antibacterial activity using electrical stimulations from polypyrrole-graphene oxide triboelectric nanogenerator. *Nano Energy.* 2023;112:108463.

doi: 10.1016/j.nanoen.2023.108463

6. Khan M, Khurram AA, Li T, *et al.* Synergistic effect of organic and inorganic nanofillers on the dielectric and mechanical properties of epoxy composites. *J Mater Sci Technol.* 2018;34(12):2424-2430.

doi: 10.1016/j.jmst.2018.03.044

7. Aazem I, Mathew DT, Radhakrishnan S, *et al.* Electrode materials for stretchable triboelectric nanogenerator in wearable electronics. *RSC Adv.* 2022;12(17):10545-10572.

doi: 10.1039/D2RA00017B

8. Lee K, Sahu M, Hajra S, Mohanta K, Kim HJ. Effect of sintering temperature on the electrical and gas sensing properties of tin oxide powders. *Ceram Int.* 2021;47(16):22794-22800.

doi: 10.1016/j.ceramint.2021.05.050

9. Rabenok EV, Novikov GF, Bogdanova LM, Bukichev YS, Dzhardimalieva GI. Temperature dependence of direct current conductivity in TiO_2/epoxy polymer dielectric nanocomposites. *Russ J Phys Chem A.* 2023;97(1):186-192.

doi: 10.1134/S0036024423010200

10. Sorin ES, Baimuratova RK, Uflyand IE, *et al.* New self-healing metallosupramolecular copolymers with a complex of cobalt acrylate and 4'-phenyl-2,2':6',2"-terpyridine. *Polymers (Basel).* 2023;15(6):1472.

doi: 10.3390/polym15061472

11. Behera SA, Hajra S, Panda S, Amanat A, Achary PGR. Structural and electrical properties of 0.98($K0.5Na0.5NbO_3$)-0.02($Bi0.5Na0.5TiO_3$) ceramics. *J Met Mater Miner.* 2023;33(4):1894.

12. Bunriw W, Harnchana V, Chanthad C, *et al.* TiO_2/Ag hybrid filler with synergistic effect of dielectric modulation and photocharge generation in natural rubber-based triboelectric nanogenerator. *Mater Res Bull.* 2025;193:113682.

doi: 10.1016/j.materresbull.2024.113682

13. Wang J, Liu S, Wang J, Hao H, Zhao L, Zhai J. Improving dielectric properties and energy storage performance of PVDF nanocomposite by surface-modified $SrTiO_3$ nanoparticles. *J Alloys Compd.* 2017;726:587-592.

doi: 10.1016/j.jallcom.2017.07.029

14. Wang ZL, Wang AC. On the origin of contact-electrification. *Mater Today.* 2019;30:34-51.

doi: 10.1016/j.mattod.2019.05.016

15. Wang S, Lin L, Wang ZL. Triboelectric nanogenerators as self-powered active sensors. *Nano Energy.* 2015;11:436-462.

doi: 10.1016/j.nanoen.2014.10.034

16. Parimalam M, Islam MR, Yunus RM. Effects of nanosilica, zinc oxide, and titanium oxide on the performance of epoxy hybrid nanocoating. *Polym Test.* 2018;70:197-207.

doi: 10.1016/j.polymertesting.2018.07.017

17. Noman MT, Ashraf MA, Ali A. Synthesis and applications of nano-TiO2: A review. *Environ Sci Pollut Res Int.* 2019;26:3262-3291.

doi: 10.1007/s11356-018-3877-6

18. Pandey P, Thapa K, Ojha GP, *et al.* Metal-organic frameworks-based triboelectric nanogenerator powered visible light communication system for wireless human-machine interactions. *Chem Eng J.* 2023;452:139209.

doi: 10.1016/j.cej.2022.139209

19. Patsidis A, Psarras GC. Dielectric behaviour and functionality of polymer matrix-ceramic $BaTiO_3$ composites. *Express Polym Lett.* 2008;5(10):691-701.

doi: 10.3144/expresspolymlett.2008.86

20. Prateek TV, Kumar V. Recent progress on ferroelectric polymer-based nanocomposites for high energy density capacitors: Synthesis, dielectric properties, and future aspects. *Chem Rev.* 2016;116(7):4260-4317.

doi: 10.1021/acs.chemrev.5b00361

21. Babu A, Bochu L, Potu S, *et al.* Facile direct growth of ZIF-67 metal-organic framework for triboelectric nanogenerators and their application in the Internet of Vehicles. *ACS Sustainable Chem Eng.* 2023;11(47):16806-16817.

doi: 10.1021/acssuschemeng.3c05925

22. Wu Z, Cheng T, Wang ZL. Self-powered sensors and systems based on nanogenerators. *Sensors (Basel).* 2020;20(10):2925.

doi: 10.3390/s20102925

23. Xu L, Chen Y, Yu M, *et al.* NIR light-induced rapid self-healing hydrogel toward multifunctional applications in sensing. *Nano Energy.* 2023;107:108119.

doi: 10.1016/j.nanoen.2022.108119

24. Yin L, Wang Q, Zhao H, Bai J. Improved energy density obtained in trilayered poly(vinylidene fluoride)-based composites by introducing two-dimensional BN and TiO_2 nanosheets. *ACS Appl Mater Interfaces.* 2023;15(12):16079-16089.

doi: 10.1021/acsami.2c21842

25. Wen Z, Shen Q, Sun X. Nanogenerators for self-powered gas sensing. *Nano Micro Lett.* 2017;9(4):45.

doi: 10.1007/s40820-017-0146-y

26. Islam MR, Parimalam M, Sumdani MG, Taher MA, Asyadi F, Yenn TW. Rheological and antimicrobial properties of epoxy-based hybrid nanocoatings. *Polym Test.* 2020;81:106202.

doi: 10.1016/j.polymertesting.2019.106202

27. Hanny A, Islam MR, Sumdani MG, Rashidi NM. Effects of sintering on the properties of epoxy composites reinforced with chicken bone-based hydroxyapatites. *Polym Test.* 2019;78:105987.

doi: 10.1016/j.polymertesting.2019.105987

28. Baimuratova RK, Zhinzhilo VA, Uflyand IE, *et al.* Low-temperature synthesis of metal-organic coordination polymers based on oxo-centered iron complexes: Magnetic and adsorption properties. *Russ J Phys Chem A.* 2023;97(4):735-748.

doi: 10.1134/S0036024423040109

29. Guo N, DiBenedetto SA, Tewari P, Lanagan MT, Ratner MA, Marks TJ. Nanoparticle size, shape, and interfacial effects on leakage current density, permittivity, and breakdown strength of metal oxide-polyolefin nanocomposites: Experiment and theory. *Chem Mater.* 2010;22(4):1567-1578.

doi: 10.1021/cm902560m

30. Guo R, Luo H, Liu W, *et al.* High energy density in PVDF nanocomposites using an optimized nanowire array. *Phys Chem Chem Phys.* 2018;20(26):18031-18037.

doi: 10.1039/C8CP01671A

31. Hatta FF, Mohammad Haniff MAS, Mohamed MA. A review on applications of graphene in triboelectric nanogenerators. *Int J Energy Res.* 2022;46(2):544-576.

doi: 10.1002/er.7187

32. Zha JW, Song HT, Dang ZM, Shi CY, Bai J. Mechanism analysis of improved corona-resistant characteristic in polyimide/TiO_2 nanohybrid films. *Appl Phys Lett.* 2008;93(19):192911.

doi: 10.1063/1.3037074

33. Zhang YH, Dang ZM, Xin JH, *et al.* Dielectric properties of polyimide–mica hybrid films. *Macromol Rapid Commun.* 2005;26(18):1473-1477.

doi: 10.1002/marc.200500387

34. Zheng H, Wu H, Yi Z, *et al.* Remote-controlled droplet chains-based electricity generators. *Adv Energy Mater.* 2023;13(10):2203825.

doi: 10.1002/aenm.202203825

35. Parimalam M, Islam MR, Yunus RM. Effects of nanosilica and titanium oxide on the performance of epoxy-amine nanocoatings. *J Appl Polym Sci.* 2019;136(35):47901.

doi: 10.1002/app.47901

36. Yang L, Wang H, Fang S, Li M. Research progress on energy storage performance enhancement strategies for polyvinylidene fluoride-based composites. *J Alloys Compd.* 2023;960:170831.

doi: 10.1016/j.jallcom.2022.170831

37. Yu E, Zhang Q, Xu N, Yang H. F-TiO2/P(VDF-HFP) hybrid films with enhanced dielectric permittivity and low dielectric loss. *RSC Adv.* 2017;7(7):3949-3957.

doi: 10.1039/C6RA27441C

38. Zha JW, Dang ZM, Zhou T, Song HT, Chen G. Electrical properties of TiO_2-filled polyimide nanocomposite films prepared via an *in situ* polymerization process. *Synth Met.* 2010;160(23-24):2670-2674.

doi: 10.1016/j.synthmet.2010.09.008

39. Bukichev YS, Bogdanova LM, Spirin MG, Shershnev VA, Shilov GV, Dzhardimalieva GI. Composite materials based on epoxy matrix and titanium dioxide (IV) nanoparticles: Synthesis, microstructure and properties. *Metallurgy.* 2021;28(2):224-237.

40. Chen X, Mao SS. Titanium dioxide Nanomaterials: Synthesis, properties, modifications and applications. *Chem Rev.* 2007;107:2891-2959.

doi: 10.1021/cr0500535

41. Van de Lagemaat J, Park NG, Frank AJ. Influence of electrical potential distribution, charge transport, and recombination on the photopotential and photocurrent conversion efficiency of dye-sensitized nanocrystalline TiO_2 solar cells. *J Phys Chem B.* 2000;104(9):2044-2050.

doi: 10.1021/jp993803d

42. Zaban A, Meier A, Gregg BA. Electric potential distribution and short-range screening in nanoporous TiO_2 electrodes. *J Phys Chem B.* 1997;101(40):7985-7991.

doi: 10.1021/jp973142f

43. Liu H, Feng Y, Shao J, *et al.* Self-cleaning triboelectric nanogenerator based on TiO_2 photocatalysis. *Nano Energy.* 2020;70:104499.

doi: 10.1016/j.nanoen.2020.104499

44. Yadav P, Sahay K, Srivastava M, Verma A, Yadav BC. Emerging trends in self-healable nanomaterials for triboelectric nanogenerators: A comprehensive review and

roadmap. *Front Energy.* 2023;17:1-24.

doi: 10.1007/s11708-023-0896-2

45. Yadav P, Sahay K, Verma A, Maurya DK, Yadav BC. Applications of multifunctional triboelectric nanogenerator (TENG) devices: Materials and prospects. *Sustain Energy Fuels.* 2023;7(16):3796-3831.

doi: 10.1039/D3SE00788E

46. Park H-W, Huynh ND, Kim W, *et al*. Effects of embedded TiO_{2-x} nanoparticles on triboelectric nanogenerator performance. *Micromachines.* 2018;9(8):407.

doi: 10.3390/mi9080407

47. Bhatta S, Mitra R, Ramadoss A, Manju U. Enhanced voltage response in TiO_2 nanoparticle embedded piezoelectric nanogenerator. *Nanotechnology.* 2022;33(33):335402.

doi: 10.1088/1361-6528/ac8bda

48. Yu X, Han X, Zhao Z, *et al*. Hierarchical TiO_2 nanowire/graphite fiber photoelectrocatalysis setup powered by a wind-driven nanogenerator: A highly efficient photoelectrocatalytic device entirely based on renewable energy. *Nano Energy.* 2015;11:19-27.

doi: 10.1016/j.nanoen.2014.11.009

49. Kulkarni ND, Kumari P. Development of highly flexible PVDF-TiO_2 nanocomposites for piezoelectric nanogenerator applications. *Mater Res Bull.* 2023;157:112039.

doi: 10.1016/j.materresbull.2022.112039

50. Bunriw W, Harnchana V, Chanthad C, Huynh VN. Natural rubber-TiO_2 nanocomposite film for triboelectric nanogenerator application. *Polymers (Basel).* 2021;13(13):2213.

doi: 10.3390/polym13132213

51. Huo Z, Kim YJ, Chen Y, *et al*. Hybrid energy harvesting systems for self-powered sustainable water purification by harnessing ambient energy. *Front Environ Sci Eng.* 2023;17(10):118.

52. Alam MM, Sultana A, Mandal D. Biomechanical and acoustic energy harvesting from TiO_2 nanoparticle modulated PVDF nanofiber made high performance nanogenerator. *ACS Appl Energy Mater.* 2018;1(7):3103-3112.

doi: 10.1021/acsaem.8b00613